Thin Solid Films 520 (2011) 18–24

Contents lists available at ScienceDirect

Thin Solid Films

journal homepage: www.elsevier.com/locate/tsf

In situ preparation of Calcium hydroxide films

S. Dahle [a], F. Voigts [a], W. Maus-Friedrichs [a,b,*]

[a] Institut für Physik und Physikalische Technologien, Technische Universität Clausthal, Leibnizstrasse 4, 38678 Clausthal-Zellerfeld, Germany
[b] Clausthaler Zentrum für Materialtechnik, Technische Universität Clausthal, Leibnizstrasse 4, 38678 Clausthal-Zellerfeld, Germany

ARTICLE INFO

Article history:
Received 4 August 2010
Received in revised form 11 April 2011
Accepted 13 April 2011
Available online 22 April 2011

Keywords:
Metastable Induced Electron Spectroscopy
Ultraviolet Photoelectron Spectroscopy
X-ray Photoelectron Spectroscopy
Calcium
Calcium oxide
Calcium hydroxide
Water
Hydrogen

ABSTRACT

The in situ preparation of Calcium hydroxide films in an ultra high vacuum (UHV) is constrained by the decomposition of species at the surface and the absence of OH bulk diffusion. Therefore, it is not possible to prepare such films simply by water exposure to a Calcium layer.
We present four different approaches for the preparation of $Ca(OH)_2$ films in an UHV. Two of these methods are found to be ineffective for the preparation, the other two are shown to produce Calcium hydroxide films. Both of the two effective procedures make use of H_2 gas exposure. Metastable Induced Electron Spectroscopy, Ultraviolet Photoelectron Spectroscopy, and X-ray Photoelectron Spectroscopy are employed to verify quality and purity of the films.

1. Introduction

The interaction of Calcium hydroxide with different gases and liquids is of great technological importance. Among the applications are for example the use of limestone for desulphurisation at industrial processes e.g. at the Giulini process employing Calcium hydroxide to produce gypsum [1] or the preparation of Calcium hypochlorite out of suspensions of Calcium hydroxide [2]. Another promising application is the use of $Ca(OH)_2$ as chemical heat pump and storage [3,4]. A better understanding of the reaction kinetics of $Ca(OH)_2$ may lead to a significant improvement of the applications. Even the carbonation process of burnt limestone used as plaster is not fully understood. Although the behavior of hydrated limestone has been investigated for more than one century in materials science [5], fundamental investigations on the underlying processes leading to the behavior of the different types of hydrated lime are missing. There are a few microscopic approaches on the hydration of burnt limestone [6], but none of them gives insight neither on the microscopic processes nor the following carbonation. Most of the investigations on the hydration or carbonation of Calcium oxide propose the generation of surface product layers or films [6,7], which appears to be quite convincing. These films act as barriers later on, while dissociation processes at the surfaces of these films may improve diffusion and reaction rates. Therefore, an investigation on this topic should start determining surface processes. Afterwards the results can be extended to bulk processes and the effect of the solid–liquid–interfaces. Studies on all of the given issues have to start with a well understood and clean prepared system, i.e. under vacuum conditions. As a first step, the preparation of the samples has to be developed. The investigations require film thicknesses of several nm at least with qualities at least as good as the industrial $Ca(OH)_2$ powder used as reference.

In this paper four methods for the preparation of Calcium hydroxide films in an ultra high vacuum are presented. Quality and purity of the films are confirmed by means of Metastable Induced Electron Spectroscopy (MIES) and Ultraviolet Photoelectron Spectroscopy (UPS) measurements complemented by X-ray Photoelectron Spectroscopy (XPS).

The interpretation of all results presented here mainly bases on our previously published results on the interaction of Calcium surfaces with oxygen and water [8] as well as on published results from other groups. Dupin et al. [9] investigated CaO and $Ca(OH)_2$ samples beside others with XPS and compared their results with Extended Hückel theory-tight binding calculations. Sosulnikov et al. [10] investigated Ca metal samples freshly prepared under vacuum conditions, later on oxidized them at above 600 K and compared the results with natural $CaCO_3$. All these results have been summarized in Table 1. The exact binding energies given in these publications slightly vary, which may be due to insufficient compensation of charging effects.

The chemical shift of the Ca-induced peaks during interaction with the different gases in XPS is beyond the resolution of our experimental setup. Therefore, no spectrum of the Ca XPS peaks is shown, although

* Corresponding author at: Institut für Physik und Physikalische Technologien, Technische Universität Clausthal, Leibnizstrasse 4, 38678 Clausthal-Zellerfeld, Germany. Tel.: +49 5323 72 2310; fax: +49 5323 72 3600.
E-mail address: w.maus-friedrichs@pe.tu-clausthal.de (W. Maus-Friedrichs).

0040-6090/$ – see front matter © 2011 Elsevier B.V. All rights reserved.
doi:10.1016/j.tsf.2011.04.088

Table 1
Comparison of XPS results from several workgroups for Calcium oxide and hydroxide used as input parameters for the mathematical fit.

Reference	Ca $2p_{3/2}$	Oxidic O 1s Gaussian		Hydroxidic O 1s Gaussian	
	Binding energy in eV	Binding energy in eV	Binding energy relative to Ca $2p_{3/2}$ in eV	Binding energy in eV	Binding energy relative to Ca $2p_{3/2}$ in eV
Bebensee et al. [8]	348.6	531.4	182.8	533.5	184.9
Dupin et al. [9]	346.3	528.5	182.2	530.8	184.5
Sosulnikov et al. [10]	346.0	528.9	182.9		

we apply the Ca $2p_{3/2}$ peak as a reference for the compensation of charging effects. This is done by discussing binding energy differences rather than the absolute values.

A possible method to produce films of $Ca(OH)_2$ has been described in a previous work on the adsorption of water on Ca and CaO films [8]. However, this method applied water dosages of more than 10^{11} L, making it an ex situ method. These results have therefore only been taken into account to gain reference values for the peak widths used for interpretation.

2. Experimental details

An ultra high vacuum apparatus with a base pressure of 5×10^{-11} hPa, which has been described in detail previously [11], is used to carry out the experiments. All measurements were performed at room temperature.

Electron spectroscopy is performed using a hemispherical analyzer (VSW HA100) in combination with a source for metastable helium atoms (mainly $He^*\ ^3S_1$) and ultraviolet photons (HeI line). A commercial non-monochromatic X-ray source (Specs RQ20/38C) is utilized for XPS.

During XPS, X-ray photons hit the surface under an angle of 80° to the surface normal, illuminating a spot of several mm in diameter. For all measurements presented here, the Al K_α line with a photon energy of 1486.7 eV is used. Electrons are recorded by the hemispherical analyzer with an energy resolution of 1.1 eV under an angle of 10° to the surface normal. All XPS spectra are displayed as a function of binding energy with respect to the Fermi level.

For quantitative XPS analysis, photoelectron peak areas are calculated via mathematical fitting with Gauss-type profiles using OriginPro 7G including the peak fitting module, which applies Levenberg–Marquardt algorithms to achieve the best agreement possible between experimental data and fit. Due to the plain background observed for the Ca 2p and O 1s structures, a linear background subtraction was applied before the fitting procedure. Peak widths (full width at half maximum, FWHM) and binding energies from preliminary experiments on CaO and $Ca(OH)_2$ [8] are used as input parameters for the fits. A FWHM of 1.8 eV is used for the oxidic Gaussian and of 2.75 eV for the hydroxidic Gaussian. The binding energy difference between these two has been fixed to 2.0 eV. This value has been determined by comparing adsorption experiments [8] to literature [9,10] as shown in Table 1. Photoelectric cross sections as calculated by Scofield [12] and inelastic mean free paths from the NIST database [13] as well as the energy dependent transmission function of our hemispherical analyzer are taken into account when calculating stoichiometry.

MIES and UPS are performed applying a cold cathode gas discharge via a two-stage pumping system. A time-of-flight technique is employed to separate electrons emitted by He* (MIES) from those caused by HeI (UPS) interaction with the surface. The combined He*/HeI beam strikes the sample surface under an angle of 45° to the surface normal and illuminates a spot of approximately 2 mm in diameter. The spectra are recorded simultaneously by the hemispherical analyzer with an energy resolution of 220 meV under normal emission within 150 s.

MIES is an extremely surface sensitive technique probing solely the outermost layer of the sample, because the He* atoms interact with the surface typically 0.3 to 0.5 nm in front of it. This may occur via a number of different mechanisms depending on surface electronic structure and work function, as described in detail elsewhere [14–16]. Only the processes relevant for the spectra presented here shall be discussed shortly.

During Auger Deexcitation (AD) an electron from the sample fills the 1s orbital of the impinging He*. Simultaneously, the He 2s electron carrying the excess energy is emitted. The resulting spectra reflect the Surface Density of States (SDOS) directly. AD-MIES and UPS can be compared and allow a distinction between surface and bulk effects. AD takes place for all systems shown here.

For low work functions below about 2.2 eV, the resonant transfer of an electron from the surface to the 2s orbital of the impinging He* atom becomes sufficiently probable. This results in a He^{*-} ($1s^12s^2$) ion in front of the sample surface which decays via an autodetachment (AU) process into its ground state very quickly [17]. Hereby, one 2s electron undergoes a transition into the 1s level while the other 2s electron is emitted carrying the excess energy. This process produces an additional sharp structure near a kinetic energy of about 19 eV with a FWHM of 0.7 eV within the AD spectrum.

All MIES and UPS spectra are displayed as a function of the electron binding energy with respect to the Fermi level. The surface work function can be determined from the high binding energy onset of the MIES or the UPS spectra with an accuracy of ±0.1 eV.

Calcium (Sigma-Aldrich, 99%) was evaporated with a commercial UHV evaporator (Omicron EFM3) onto our samples. On a clean Si (100) target metallic Calcium films grow at a rate of 0.85 nm min^{-1} at room temperature when evaporated with an Ca^+ ion flux of 500 nA at the fluxmeter of the EFM3. This flux is a measure of the number of Ca atoms moving towards the sample per second. The film growth rates for Ca and CaO have been estimated from the Si 2p peak attenuations in XPS, respectively.

CaO films were prepared by evaporation of Ca at a flux of 500 nA corresponding to a CaO growth rate of 0.45 nm min^{-1} on Si(100) in an oxygen partial pressure of 6.7×10^{-7} hPa for 900 s at a target temperature of 670 K. Temperature and oxygen pressure are subsequently held for two minutes after stop of Ca evaporation. This procedure results in Calcium oxide films of about 6.8 nm thickness [8].

H_2 (Linde Gas, 99.999%), O_2 (Linde Gas, 99.995%) and H_2O (deionized) are offered via backfilling the chamber using a bakeable leak valve. The gas line is evacuated and can be heated in order to ensure cleanness. Additionally, a cold-trap is installed to minimize water contamination during gas dosage. A quadrupole mass spectrometer (Balzers QMS 112A) is used to monitor the partial pressure of the reactive gases simultaneously during all MIES and UPS measurements.

Additional XPS experiments (not shown here) on CaO and $Ca(OH)_2$ powder samples were performed to allow clear identification of the oxygen contributions in XPS. The oxide and hydroxide samples were produced by pressing powder (Alfa Aesar, CaO 99.95%, $Ca(OH)_2$ 95.0%) with 3×10^7 Pa thus obtaining tablet samples.

3. Results and discussion

For the following discussion of the quality of the produced $Ca(OH)_2$ films, XPS reference data for comparison are necessary. The binding energies found in the literature slightly vary [18], whereas the experimental setup and resolution used are not quite well reported in most publications, though depending on the FWHM. These arguments

request for own references. Therefore we start our investigations with a $Ca(OH)_2$ powder sample prepared as described in Section 2. Due to strong charge-up effects MIES and UPS results could not be achieved, nor are any reliable literature results available. Since the XPS data is shifted through charging, the Ca $2p_{3/2}$ peak is used as a reference as described in Section 2, thus discussing only binding energy differences. The results for ex situ prepared powder samples suffer from significant surface contaminations. In our case, these are mainly carbonate groups. Nevertheless, we have been able to see the underlying hydroxide with XPS (not shown here) and provide the gained positions for comparison.

The description and discussion of the results start with the adsorption of Calcium on H_2O saturated Ca surfaces. This is necessary to investigate the feasibility to produce a $Ca(OH)_2$ film by an alternating Ca and H_2O offer. In addition, these results will be helpful to discuss the findings of the following experiment, which is the simultaneous coadsorption of Calcium and water. As different approach to both of these, we then discuss the adsorption of hydrogen on Calcium oxide films and finally the simultaneous coadsorption of Calcium, hydrogen and water.

Even though we do not show spectra of powder samples in this paper, we give the values obtained for $Ca(OH)_2$ powder in Table 2 among the experimental results of the following sections. The powder sample's data is shifted due to charging, therefore we discuss only the relative binding energies between the Ca $2p_{3/2}$ peak and the O 1s structures, as described in the experimental section.

3.1. Adsorption of Ca on H_2O saturated Ca surfaces

Fig. 1 shows MIES (a) and UPS (b) spectra of a H_2O saturated (14 L) Ca film (black line). The film thickness amounts to 0.8 nm which was estimated by the attenuation of the Si 2p signal from the underlying substrate in XPS as described in the experimental. The work function of this surface amounts to 2.7 eV. Both MIES and UPS show a peak doublet at binding energies of 7.6 eV and 11.8 eV, the MIES spectrum is due to the AD process [14,15]. This doublet is the well known fingerprint of surface OH groups corresponding to the OH molecular orbitals 1π and 3σ [19]. Beside these peaks UPS shows an additional contribution at 5.5 eV. This corresponds to electrons emitted from O 2p derived orbitals from the underlying CaO film. It is well known, that H_2O interacts with Ca surfaces in a two step mechanism [8]:

1. On pure and only partly covered Ca surfaces the impinging H_2O molecules are completely dissociated. The remaining oxygen is incorporated into the Ca film building CaO clusters. The remaining H atoms are most likely desorbed as H_2 molecules after recombination. These processes take place as long as the surface shows metallic properties from occupied Ca 4s orbitals.
2. The increasing H_2O exposure results in a decreasing electron density just below the Fermi level which results in a decreasing probability for the complete H_2O dissociation. This means that further impinging H_2O molecules are only partly dissociated forming H atoms and OH molecules. Subsequently, both take part in the formation of surface OH groups. All processes end up when the surface is completely covered with OH groups.

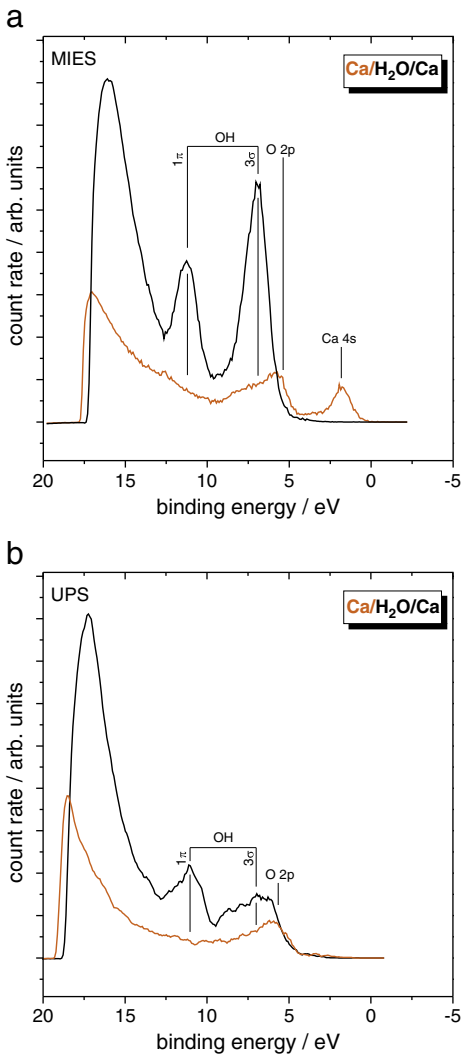

Fig. 1. MIES (a) and UPS (b) spectra of a Ca film exposed to water (4.8×10^{-9} hPa for 65 min corresponding to a H_2O exposure of 14 L) without (black line) and with (orange line) additional Ca adsorption.

The H_2O saturated Ca surface shows a complete OH covered surface with an underlying CaO film. This is visible in the MIES and UPS spectra shown here.

Table 2
XPS results from the O 1s region. Values shown in bold letters as well as the binding energy difference between peak I and II are constraints used for the fitting procedure.

System	Figure	Peak	Binding energy relative to Ca $2p_{3/2}$ in eV	Absolute binding energy values in eV	FWHM in eV	Relative intensity	Assignment
$Ca(OH)_2$ powder	Not shown	II	184.4	536.9	**2.75**	0.95	Hydroxide
		III	186.9	539.4	1.76	0.05	–
Ca evaporation in a H_2O atmosphere	3	I	182.0	530.1	**1.80**	0.47	Oxide
		II	184.0	532.1	**2.75**	0.38	Hydroxide
		IIIa	184.9	533.0	1.88	0.15	–
H_2 exposure to a CaO film	6	I	181.8	530.3	**1.8**	0.01	Oxide
		II	183.8	532.3	**2.75**	0.94	Hydroxide
		IIIb	186.3	534.8	2.33	0.05	–
Ca evaporation in a combined H_2O and H_2 atmosphere	8	I	182.0	530.8	**1.80**	0.02	Oxide
		II	184.0	532.8	**2.75**	0.98	Hydroxide

Adsorbing further Ca atoms (corresponding to an entire film thickness of about 1.9 nm) leads to a complete change of the peak structure (orange lines in Fig. 1). The work function of this surface amounts to 2.0 eV. Both MIES and UPS show O 2p emission at 5.5 eV. OH is completely vanished in UPS and almost completely vanished in MIES. Furthermore, a peak denoted by Ca 4s appears which is due to the AU contributions as well as the AD process. AU is only possible if the work function is below about 2.2 eV [8,14–16] and if the SDOS of the sample exhibits metallic character, i.e. occupied Ca 4s states just below the Fermi level. Both conditions appear to be fulfilled here. The probability of each process is a function of the SDOS and the work function. The detail composition of the Ca 4s contribution formed by AD and AU processes has been discussed previously [8]. It should be mentioned that Ca 4s emission is not visible in UPS due to the very small photoionization cross section with s-like orbitals for HeI UV radiation [20].

The repeated alternating adsorption of Ca films (thicknesses of about 1.0 nm) followed by H_2O exposure (14 L) suffers from the problem, that the Ca offer to the $Ca(OH)_2$ surface obviously results in the complete decomposition of at least the surface layer probably following this reaction scheme:

$$Ca + Ca(OH)_2 \rightarrow 2\cdot CaO + H_2 + 284.6\,\frac{kj}{mol}.$$

The value for the binding enthalpy follows Lide et al. [21]. Any alternating offer of Ca and H_2O is therefore not able to produce $Ca(OH)_2$ films thicker than one layer. Summarizing, we find that the adsorption of Ca atoms on $Ca(OH)_2$ surface layers results in the complete decomposition of the hydroxyl groups and the formation of a surface oxide.

3.2. Evaporation of Ca during water exposure

Fig. 2 shows MIES (black line) and UPS (orange line) spectra obtained after Ca exposure to a Si(100) target at a flux of 100 nA in an atmosphere consisting of 1.0×10^{-6} hPa of H_2O for 15 min (corresponding to 680 L). The Ca exposure generates a film growth of about 0.34 nm/min according to a final film thickness of 5.1 nm (corresponding to 13 L H_2O per nm). MIES again shows the well known OH orbitals 1π and 3σ at binding energies 7.6 eV and 11.8 eV. In contrast, UPS shows the O 2p emission at 5.5 eV and an additional structure which may be due to surface contaminations like CO_3^{2-}. This additional structure can just hardly be seen in the MIES spectrum where solely adsorbed hydroxyl groups are seen. It is likely to assume, that these structures are produced by hydrocarboneous layers consisting of OH groups terminating the surfaces.

Fig. 3 shows the XPS spectrum from the O 1s range for the simultaneous H_2O and Ca exposure corresponding to Fig. 2. The original data is shown as black dots, the mathematical fit as described in Section 2 is shown as a solid red line. The single Gaussians are shown as dashed blue lines. For better comparability, the O 1s contributions are consistently denoted as I for the oxide, II for the hydroxide and III for any third species in all XPS spectra. We find the oxidic peak (I) with 55% of the overall intensity of the O 1s structure at a binding energy of 530.1 eV and the hydroxidic peak (II) with a fraction of 45% at a binding energy of 532.1 eV. Besides these, a third peak (IIIa) is found at a binding energy of 533.0 eV with a FWHM of 1.9 eV. The relative binding energies shown in Table 2 fit quite well to the preliminary results [8] as well as to the results for the powder sample. The intensity distribution over the three species indicates a prevalence of the oxide.

The procedure described here suffers from the same problem as the alternating film production (Section 3.1) that the impinging Ca atoms decompose surface hydroxides. Nevertheless, due to statistical absorption and diffusion some hydroxide is found, but can never be sufficiently pure. The third O 1s peak (IIIa) found at a binding energy beyond the hydroxide fits very well to preliminary results for Calcium carbonate [22]. The additional peak in the UPS spectrum (at about 14 eV in Fig. 2) supports this assumption as well as the presence of a C 1s peak in the XPS survey spectrum (not shown here). It follows that this preparation method is not able to produce neither $Ca(OH)_2$ films nor layers in sufficient quality.

3.3. Adsorption of H_2 on a CaO film

Fig. 4 shows MIES (a) and UPS spectra (b) of a CaO film with a thickness of 1.3 nm prepared as described in Section 2 during exposure to H_2 up to an offer of 425 L. For easy comparison and tracking of the peak evolution, the spectra are displayed with an offset in a waterfall manner. The respective actual dosage is indicated by the arrow at the right side of the spectra, starting at the bottom with an exposure of 0 L. During H_2 offer the work function increases from 2.1 eV to 2.8 eV. The pure CaO (bottom spectrum) shows O 2p contributions at a binding energy of 5.5 eV in MIES and UPS. Furthermore, we find some contributions at higher binding energies corresponding to a slight

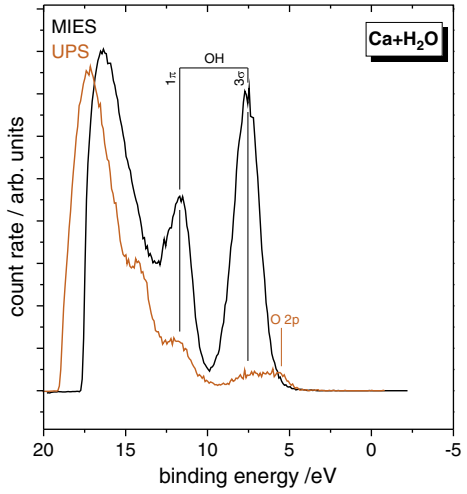

Fig. 2. MIES (black line) and UPS (orange line) spectra of a Ca film evaporated in an atmosphere of 1.0×10^{-6} hPa H_2O, the UPS spectrum has been scaled up linearly to match the size of the MIES spectrum.

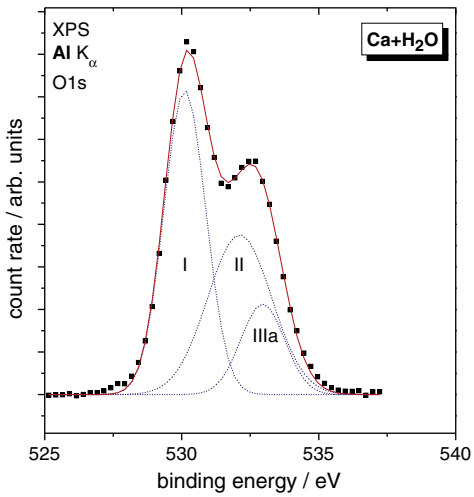

Fig. 3. XPS spectrum of the O 1s region of a Ca film evaporated in an atmosphere of 1.0×10^{-6} hPa H_2O (corresponding to Fig. 2).

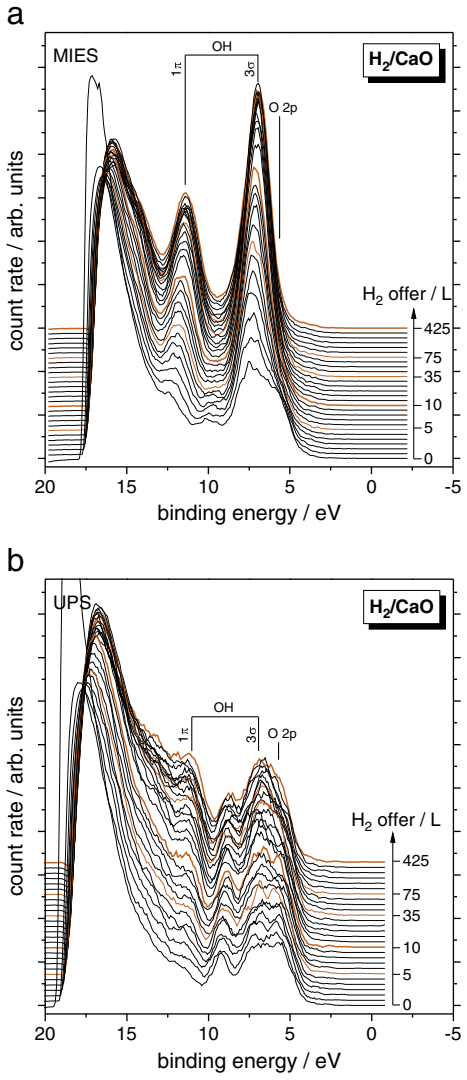

Fig. 4. MIES (a) and UPS (b) spectra of a CaO film during H_2O offer up to 425 L.

surface contamination, most of them being due to OH groups. These contaminations do not influence the further experiment as most of the surface remains oxidic until the start of the experiment. Furthermore, the surface oxides readily form hydroxide with any impinging hydrogen, thus matching to the initial hydroxide contamination. The exposure to H_2 results in the formation of OH. While MIES does not show O 2p any more even at a very small exposure of 10 L of H_2 (thick orange line), it requires more than 400 L of H_2 to achieve saturation in UPS. At 425 L (top spectrum) we find a clearly visible OH formation in UPS, but a smaller contribution of the O 2p corresponding to CaO remains.

Fig. 5 shows the evolution of the work function (black circles and solid black line) and the intensity of the OH 3σ MIES structure (orange triangles) during H_2 offer on a CaO film. At first, we find a conjoined behavior of MIES peak intensity and work function. At about 45 L the MIES peak intensity reaches its maximum. The surface work function slightly increases beyond further 45 L reaching its saturation value of 3.1 eV only at about 400 L. This gives evidence for the occurrence of bulk effects, which barely influence the MIES intensity in contrast to the work function. The initial value of the work function is 2.0 eV which is 0.3 eV higher than found for pure oxides [8]. This may be due to initial hydroxide formation from the residual gas. The final value of 3.1 eV is 0.4 eV higher than found for $Ca(OH)_2$ surface layers. Since the MIES signal depends only on the outermost layer of the surface and

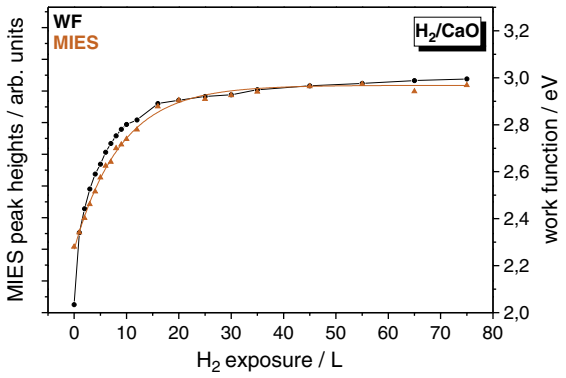

Fig. 5. MIES peak height analysis for the OH 3σ structure from Fig. 4 (orange triangles) with a Langmuir isotherm fit (orange line) and surface work function (black circles and black line) of a CaO film plotted as a function of H_2 exposure.

because we can neglect decomposition of the hydroxide species formed during the reaction, we assume a Langmuir isotherm model for the chemisorption of the H_2 molecules on the surface. Fitting the Langmuir isotherm model equation to our data yielded the following correlation for the MIES OH 3σ structure intensity I(D) dependence on the H_2 dosage D (in Langmuir) as follows:

$$I(D) \propto 1 - \exp\left[-\frac{(D + 2.894\,L)}{8.85\,L}\right].$$

The result of the fit is displayed as the orange line in Fig. 5. It matches the experimental results very well.

Fig. 6 shows the XPS spectrum from the O 1s range for the H_2 saturated CaO surface corresponding to Fig. 4. We find peak (I) with a fraction near the resolution limit at a binding energy of 530.3 eV, the main contribution (II) at 532.3 eV and a third one (IIIb) at 534.8 eV with a FWHM of 2.33 eV. Different peak positions compared to the other samples are due to a charge-up appearing for the XPS measurements on insulating films while peak IIIb may be due to a different chemical species compared to peak IIIa after the water dosage. The relative binding energy distances of these O 1s peaks to the corresponding Ca $2p_{3/2}$ peak are shown in Table 2. The values are quite similar and fit well to our preliminary results for the adsorption of water on CaO [8].

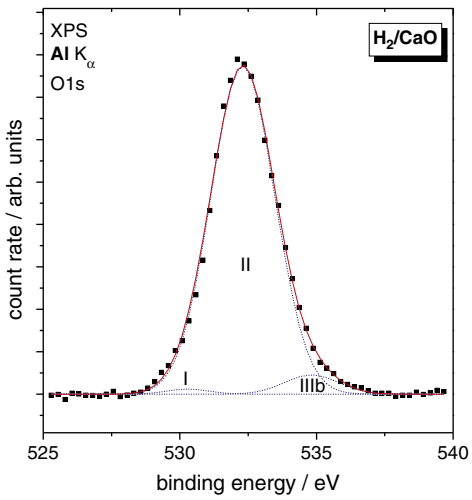

Fig. 6. XPS spectrum of the O 1s region of a CaO film exposed to 425 L H_2 (corresponding to the top spectra in Fig. 4).

The chemical shift of 2.5 eV between species II and IIIb is higher than the shift found for carbonates [22]. Since we found a similar feature for the powder sample, this method apparently resembles a $Ca(OH)_2$ film. This seems to be quite unlikely at the first glance, because the reaction of CaO and H_2 to $Ca(OH)_2$ lacks one oxygen atom per molecule. Film thicknesses of about 1.4 nm before and about 1.3 nm after the dosage of H_2 exclude any significant loss of Calcium atoms during the interaction as the main process to compensate the lack of oxygen.

The reaction described above was affected by unavoidable water pollution from the residual gas as measured by quadrupole mass spectrometry performed during all gas adsorption experiments. The residual water amounted to about 5% during H_2 exposure that leads to a total dosage of 23 L of H_2O corresponding to about 4 L per monolayer. Even though the water content was not meant to be offered, the influence of the residual gas is unavoidable. We assume that the water from the residual gas is required for the reaction. Following our previously published results for the interaction of H_2O molecules with Ca films [8], this offer is sufficient to completely oxidize a film of metallic Calcium. Assuming an enhanced diffusion of defects in the produced film, this content of water may also be the oxygen source at our reaction. Taking into account the most probably unordered surface, we assume the dissociation of hydrogen at surface defects followed by a diffusion of the hydrogen atoms into the film and a formation of defects by the hydrogen. This kind of defect could have diffusivities large enough to migrate back to the surface to get compensated. Therefore we propose a reaction scheme as follows (we apply Kröger–Vink notation for the bulk structures only [23]):

$$O_o^x + \frac{1}{2}H_2 \rightarrow (OH)_o^{\cdot} + e'$$

$$V_o^{\cdot\cdot} + e' + H_2O \rightarrow (OH)_o^{\cdot} + \frac{1}{2}H_2\uparrow.$$

Summing up both steps the hydrogen enables the reaction throughout the whole film. Regarding the spectra during the hydrogen dosage, we find an additional peak at about 9 eV in UPS and about 10 eV in MIES. This peak cannot be identified definitely, but it does not fit to any Ca containing species measured until now. On the other hand, the position fits quite well to all hydride species measured so far [24–26]. This indicates that part of the Ca atoms may form a species connatural to Calcium hydride.

Up to 45 L of H_2 exposure work function and MIES OH 3σ peak behave very similarly and can be described as Langmuir isotherm, as was discussed with Fig. 6. This behavior suggests that in the first step of interaction impinging H_2 molecules are dissociated and bond in a surface OH layer. This layer saturates at an exposure of 45 L, which is visible from the saturation of the MIES OH 3σ peak and the simultaneous slope change of the work function increase. Further impinging H_2 is incorporated into the CaO film subsequently. As a summary we find that hydrogen adsorption on Calcium oxide is a possible method to produce $Ca(OH)_2$ films, even though a minimum amount of water vapor seems to be necessary.

3.4. Evaporation of Ca during combined hydrogen and water exposure

Fig. 7 shows MIES (black line) and UPS (orange line) spectra obtained after Ca exposure to a Si(100) target at a flux of 500 nA in a mixed atmosphere consisting of 1.0×10^{-7} hPa of H_2O and 9.0×10^{-7} hPa of H_2 for 15 min (finally reaching 68 L H_2O and 609 L of H_2). This results in a film growth rate of about 0.09 nm/min according to a final film thickness of 1.4 nm. This combined water and hydrogen offer finally leads to a surface layer with a work function of 2.1 eV. Both in MIES and in UPS we clearly find the formation of OH groups at 7.6 eV and 11.8 eV. Similar to the results described in Section 3.1 in UPS some O 2p contribution at 5.5 eV remains but to a distinct smaller amount here.

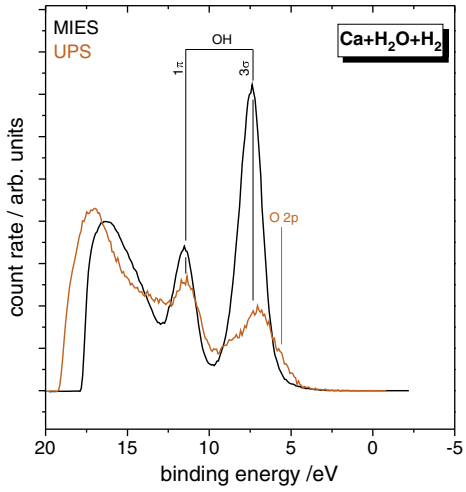

Fig. 7. MIES (black line) and UPS (orange line) spectra of a Ca film evaporated in an atmosphere of 1.0×10^{-7} hPa H_2O and 9.0×10^{-7} hPa H_2 for 15 min (corresponding to an exposure of 68 L H_2O and 609 L H_2), the UPS spectrum has been scaled up linearly to match the size of the MIES spectrum.

Fig. 8 shows the XPS spectrum from the O 1s range for the film of Ca deposited in a mixed atmosphere of H_2 and H_2O corresponding to Fig. 7. The mathematical fit shows the first peak (I) at a binding energy of 530.8 eV besides the main peak (II) at 532.8 eV. The main peak contributes to the O 1s signal with 98% and the small peak at lower binding energy with 2%.

The simultaneous exposure of Ca, H_2O and H_2 on Si samples (rates of 1.34 nm of Ca per 15 min at a H_2O partial pressure of 1.0×10^{-7} hPa corresponding to 50 L per nm in a H_2 partial pressure of 9.0×10^{-7} hPa corresponding to 453 L per nm) employs the generation of Calcium hydroxide in a continuous process. For this purpose we used water as oxidant, since the statistical adsorption of water at a Calcium atom that is already oxidized leads to hydroxide formation whereas oxygen would have no effect. The amount of O 2p emission visible in UPS seems to be smaller than was the case in Section 3.3. In the XPS spectrum of the O 1s region, the additional feature found in Section 3.3 as well as for the powder samples is missing. The oxidic part is slightly bigger than it was for before, but even so it is small in comparison with

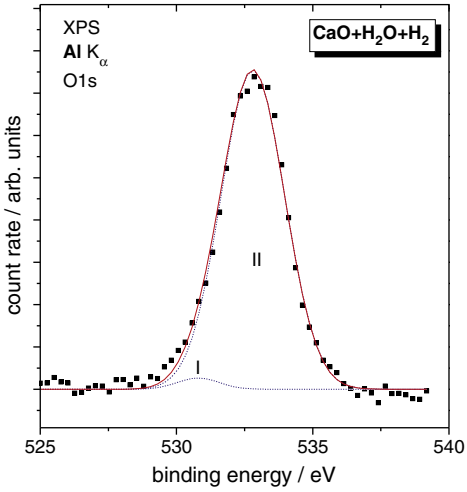

Fig. 8. XPS spectrum of the O 1s region of a Ca film evaporated in an atmosphere of 1.0×10^{-7} hPa H_2O and 9.0×10^{-7} hPa H_2 for 15 min, corresponding to an exposure of 68 L H_2O and 609 L H_2 (corresponding to Fig. 7).

the hydroxide. Taking into account all results we find that the simultaneous exposure of the CaO film to H_2O and H_2 very closely resembles a $Ca(OH)_2$ sample.

3.5. Comparison

We applied four different possible methods for the production of $Ca(OH)_2$ films under ultra high vacuum conditions. Two of them, using water to directly produce Calcium hydroxide either in a continuous process or via an alternating production route, were found to be ineffective. On the contrary, H_2 exposure is able to form Calcium hydroxide from Calcium oxide.

The two step process presented in Section 3.3 seems to be easier than the continuous method because only H_2 offer is required to saturate the previously prepared CaO film. Nevertheless, the H_2 incorporation into the CaO film will become slower with increasing CaO thickness. Up to now we are not able to give a maximum film thickness.

The continuous process presented in Section 3.4 appears to be the most promising one. Besides the fact that one has to control Ca exposure, H_2O partial pressure and H_2 partial pressure simultaneously, no limitation for maximum film thicknesses should be expected. After results of Curtis et al. [27] concerning the equilibrium constant of Calcium hydride, this species could occur on metallic Calcium during our dosage. We found a peak at a binding energy of around 10 eV in the valence band spectra that could belong to a Hydride species.

The continuous method as well as the two step process both show oxidic fractions in the XPS spectra near the resolution limit of our experimental setup. The third XPS O 1s peak found for the powder sample is visible in the film grown in two steps, but not in the continuous one. This gives evidence that the continuous method is able to produce films with fewer impurities than the two step process and the powder sample. Nevertheless, the film prepared in two steps is as pure as the powder sample, and the continuously prepared one is even cleaner. Therefore, the preconditions given in Section 1, producing a homogenous film at least as clean as commercial powder are fulfilled. The oxide contribution visible in UPS is about two times as big for the two step process as for the continuous method. All these show that the continuous method as the procedure with the simplest implementation is also able to produce films that are even cleaner than the films prepared in two steps.

4. Summary

MIES, UPS and XPS were applied to study the formation of $Ca(OH)_2$ films on Si(100) samples. Four different methods were applied, two of them were found to be working well.

One out of two working methods is a stepwise one, where we prepared a CaO film at first by evaporation of Ca at a rate of 0.45 nm min^{-1} in an oxygen partial pressure of 6.7×10^{-7} hPa at a target temperature of 670 K. Afterwards we saturated this film with H_2 at a dosage of about 100 L per monolayer.

As a continuous method we evaporated Ca at a rate of 0.09 nm min^{-1} in a hydrogen partial pressure of 9×10^{-7} hPa and a water partial pressure of 1×10^{-7} hPa, resulting in dosages of 19 L per monolayer of H_2O and 171 L per monolayer of H_2.

The preparation of $Ca(OH)_2$ solid films by both of these methods has been verified by comparison to a commercial reference ($Ca(OH)_2$ powder pressed to a sample), to previous own results for the $Ca(OH)_2$ surface layer formation on Ca films [8] as well as other groups [9,10].

Acknowledgments

The authors gratefully acknowledge valuable discussions with Dr. Harald Schmidt and technical assistance by Denise Yvonne Rehwagen.

References

[1] W. Kaminsky, Chem. Ing. Tech. 55 (1983) 667.
[2] P. Patnaik, Handbook of Inorganic Chemicals, McGraw-Hill, 2002.
[3] H. Ogura, S. Fujimoto, H. Iwamoto, H. Kage, Y. Matsuno, Y. Kanamaru, H. Nada, S. Awaya, Kagaku Kogaku Ronbun. 24 (1998) 856.
[4] H. Ogura, T. Yamamoto, H. Kage, Y. Matsuno, A.S. Mujumdar, Chem. Eng. J. 86 (2002) 3.
[5] P.E. Halstead, A.E. Moore, J. Chem. Soc. (1957) 3873.
[6] A. Wolter, S. Luger, G. Schaefer, ZKG Int. 57 (2004) 60.
[7] J.S. Dennis, R. Pacciani, Chem. Eng. Sci. 64 (2009) 2147.
[8] F. Bebensee, F. Voigts, W. Maus-Friedrichs, Surf. Sci. 602 (2008) 1622.
[9] J.-C. Dupin, D. Gonbeau, P. Vinatier, A. Levasseur, Phys. Chem. Chem. Phys. 2 (2000) 1319.
[10] M.I. Sosulnikov, Y.A. Teterin, J. Electron Spectrosc. Relat. Phenom. 59 (1992) 111.
[11] M. Frerichs, F. Voigts, W. Maus-Friedrichs, Appl. Surf. Sci. 253 (2006) 950.
[12] J.H. Scofield, J. Electron Spectrosc. Relat. Phenom. 8 (1976) 129.
[13] National Institute of Standards and Technology Electron Inelastic-Mean-Free-Path Database 1.1, http://www.nist.gov/srd/nist71.htm.
[14] Y. Harada, S. Masuda, H. Ozaki, Chem. Rev. 97 (1997) 1897.
[15] H. Morgner, Adv. At. Mol. Opt. Phys. 42 (2000) 387.
[16] G. Ertl, J. Kuppers, Low Energy Electrons and Surface Chemistry, VCH Verlag Weinheim, 1985.
[17] R. Hemmen, H. Conrad, Phys. Rev. Lett. 67 (1991) 1314.
[18] Y. Inoue, I. Yasumori, Bull. Chem. Soc. Jpn. 54 (1981) 1505.
[19] W. Maus-Friedrichs, A. Gunhold, M. Frerichs, V. Kempter, Surf. Sci. 488 (2001) 239.
[20] W.C. Price, in: C.R. Bundle, A.D. Baker (Eds.), Electron Spectroscopy: Theory, Techniques and Applications, Vol. I, Academic Press, London, 1977, p. 151.
[21] D.R. Lide, Handbook of Chemistry and Physics, 79th Edition, CRC Press, 1998.
[22] F. Voigts, F. Bebensee, S. Dahle, K. Volgmann, W. Maus-Friedrichs, Surface Science 603 (2009) 40.
[23] F.A. Kröger, H.J. Vink, Solid State Physics 3 (1956) 307.
[24] T. Komeda, Y. Sakisaka, M. Onchi, H. Kato, S. Masuda, K. Yagi, Phys. Rev. B 36 (1987) 922.
[25] M. Rogozia, H. Niehus, A. Böttcher, Surf. Sci. 519 (2002) 101.
[26] G. Lee, J.Y. Lee, J.S. Kim, Solid State Comm. 139 (2006) 516.
[27] R.W. Curtis, P. Chiotti, J. Phys. Chem. 67 (1963) 1061.